

Article

# Spatial and Temporal Changes in Temperature, Precipitation, and Streamflow in the Miyun Reservoir Basin of China

Tiezhu Yan, Zhenyao Shen \* and Jianwen Bai

State Key Laboratory of Water Environment Simulation, School of Environment, Beijing Normal University, Beijing 100875, China; yanxiaoshi1984@126.com (T.Y.); baijw@mail.bnu.edu.cn (J.B.)

\* Correspondence: zyshen@bnu.edu.cn; Tel.: +86-10-5880-0398

Academic Editor: Athanasios Loukas

Received: 11 October 2016; Accepted: 19 January 2017; Published: 28 January 2017

**Abstract:** With the influence of global climate warming, the responses of regional hydroclimatic variables to climate change are of great importance for water resource planning and management. The evolution of precipitation, mean temperature, and runoff at different timescales, was investigated using the Mann–Kendall test from 1969 to 2011 in the Miyun Reservoir Basin, China. In addition, three precipitation indices and different precipitation grades were also considered. Annual precipitation had a non-significant decreasing trend, flood precipitation trend was significantly decreasing with a magnitude of 18.50 mm/10 years, and non-flood precipitation trend was significantly increasing with a magnitude of 6.91 mm/10 years. Precipitation frequency in flood season featured a significantly decreasing trend. Meanwhile, flood precipitation intensity for large rain ( $25 \leq p < 50$  mm/day) and non-flood precipitation amount for medium rain ( $10 \leq p < 25$  mm/day) also showed significant increasing trends. The mean temperature exhibited significant upward trends during the year, in flood season, and in non-flood season with rates of 0.36 °C/10 years, 0.32 °C/10 years and 0.38 °C/10 years, respectively. The magnitude of the mean temperature increase in the non-flood season was greater than in the flood season. Runoff experienced continuous and significant downward trends of  $1.6 \times 10^8$  m<sup>3</sup>/10 years,  $1.1 \times 10^8$  m<sup>3</sup>/10 years and  $0.40 \times 10^8$  m<sup>3</sup>/10 years, respectively, during the year, in flood season, and in non-flood season. The decreased annual streamflow was more obvious after 2000 than before. The results obtained in this study could be used as references for decision-making regarding water resource management in the watershed.

**Keywords:** climate change; Miyun Reservoir Basin; precipitation structure; trend analysis; hydroclimatic variables

## 1. Introduction

Due to greenhouse gas emissions resulting from anthropogenic activities [1], global climate warming is undoubtedly happening. As supported in the Fifth Assessment Report of the Intergovernmental Panel on Climate Change (IPCC AR5), globally averaged temperature increased 0.85 °C between 1880 and 2012, and each of the last three decades has been successively warmer than any preceding decade since 1850. Global warming modifies the intensity and frequency of precipitation, which influence the hydrological cycle and the transportation and fate of pollutants, with possible adverse impact on the ecological environment [2,3]. Identifying the characteristics of regional climate change and their potential impacts on the natural system, especially at the basin scale, has therefore attracted widespread attentions from both academic circles and government. Changes in long-term hydroclimatic variables such as precipitation and temperature could represent regional climate change. To understand regional climate change impacts, it is therefore relevant to investigate the changing properties of hydroclimatic variables as the first step in the backdrop of addressing global warming [4].

At present, some studies related to trend analysis of hydroclimatic variables at watershed scale have been carried out, for example in the Lake Victoria Basin in East Africa [5], the Yellow River Basin [6], and the Three Gorges Reservoir [7]. The hydroclimatic variables analyzed generally include precipitation amount, surface air temperature, evapotranspiration, and streamflow [8–12]. The previous precipitation studies have focused mainly on changes in annual or monthly precipitation amounts and have ignored changes in precipitation structure including precipitation amount, mean precipitation intensity, and precipitation frequency. Note that changes in precipitation amount are caused by changes of precipitation frequency, precipitation intensity, or a combination of both [13,14] and that precipitation structure is a key factor in understanding the hydrologic cycle against the background of climate change [15]. Therefore, a study of changes in precipitation structure would provide a comprehensive perspective to understand precipitation variations for water resource management in the basin.

The Miyun Reservoir Basin (MRB), located in the upstream portion of the Haihe River Basin, not only plays a key role in agricultural irrigation, socioeconomic development, and eco-environment conservation in the basin, but is also a main source of drinking water for Beijing City (Figure 1). Due to climate change and human activity, streamflow into the Miyun Reservoir has decreased drastically over the past 50 years, seriously affecting Beijing’s water supply [16]. As a part of the Haihe River Basin and a typical semi-arid region in China, the regional ecological environment is sensitive to climate change as characterized by temperature and precipitation, as indicated by studies of climate change on river streamflow [16–19], water quality [20], and ecological flow [21]. Some of these studies introduced changes in annual precipitation, temperature, and runoff as a study background in the MRB. However, a comprehensive analysis of the evolution of hydroclimatic variables in the watershed has not been performed to date, let alone an analysis of precipitation structure. Nowadays, two critical questions remain unanswered: how have temperature and precipitation been changing together in space and in time over the last four decades in the Basin? How has precipitation structure around the MRB changed? The answers to these questions are very important for decision-making to ensure sustainable water resource utilization and are beneficial for providing useful baseline information for countermeasures to advance ecological restoration in the basin. This constitutes a major motivation of this study.

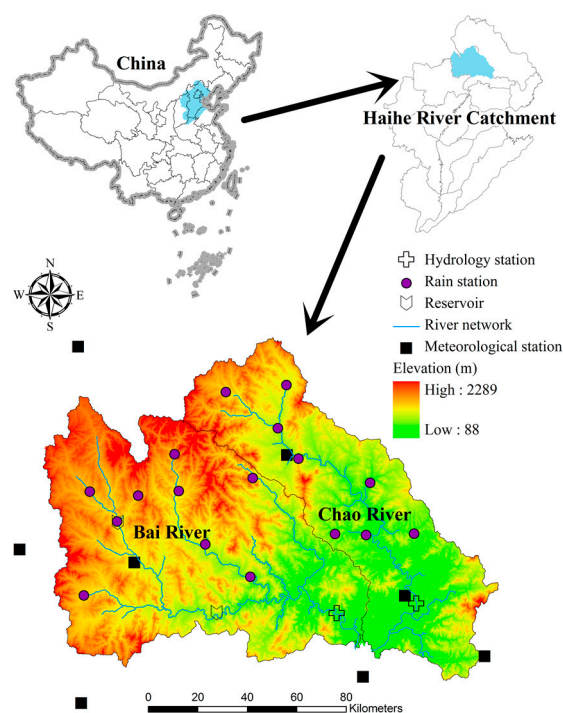


**Figure 1.** Topographical map and distribution of hydroclimatic stations in the Miyun Reservoir Basin (MRB).

Within the context of global warming, this study investigated regional responses of hydroclimatic variables (i.e., precipitation, temperature, and runoff) to climate changes in the MRB that have important implications for drinking water safety for Beijing City and the regional ecological environment. More specifically, the objectives of this study were: (1) to investigate the evolution of hydroclimatic variables in the MRB at both spatial and temporal scales over the entire basin against the background of global climate change; and (2) to understand temporal changes in precipitation structure in terms of precipitation amount, precipitation intensity and precipitation frequency for different precipitation grades. The research results lay a foundation for further research on the mechanism of future climate change in the MRB and support future planning and management of water resource by providing a strategy to maintain the health of the regional ecological environment.

## 2. Materials and Methods

### 2.1. Study Area

The Miyun Reservoir Basin (MRB), approximately 80 km away from Beijing City, China, is located between  $40^{\circ}19' N$  and  $41^{\circ}38' N$  and between  $115^{\circ}25' E$  and  $115^{\circ}35' E$ . It flows into the Miyun Reservoir, the most important surface source of drinking water for Beijing City, China. The drainage area is approximately 15,400 km<sup>2</sup>. Two tributaries, the Chao and Bai Rivers, are in the watershed (Figure 1). Watershed elevation ranges from 88 m to 2289 m. There are two major reservoirs, the Yunzhou and Baihepu reservoirs, located in the upstream and midstream portions of the Bai River, respectively (Figure 1). These two reservoirs supply agricultural irrigation for the upstream part of Miyun Reservoir. The watershed experiences a temperate continental monsoon climate that is cold and dry in winter, but rainy and hot in summer. Mean annual precipitation is about 487 mm, but precipitation is not distributed evenly throughout the year and occurs mainly in flood season (June to September), which accounts for more than 80% of total annual precipitation. In a region with precipitation-driven hydrologic processes, the internal distribution pattern of streamflow is similar to that of precipitation (Figure 2). The average annual temperature is approximately 5.7 °C [16].

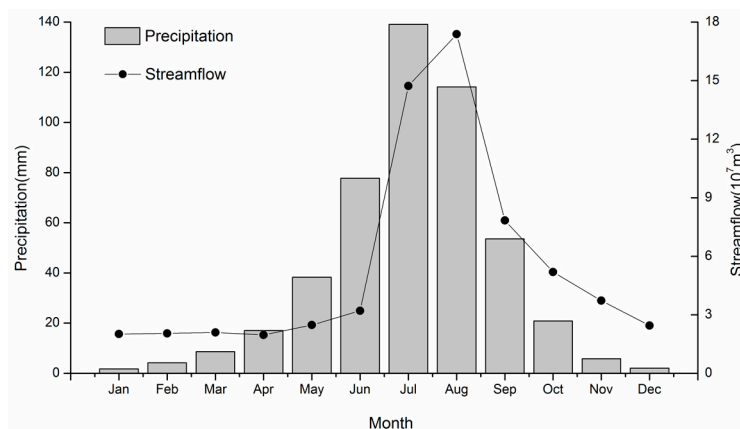


**Figure 2.** Intra-annual distributions of streamflow and precipitation from 1969 to 2011.

### 2.2. Data Acquisition and Processing

Daily precipitation data were gathered in this study from 21 rain gauges and five meteorological stations in the basin; monthly mean air temperature from nine meteorological stations in and around the basin; and monthly streamflow data from two hydrological stations. The National Climatic Center (NCC) of the China Meteorological Administration (CMA) offered precipitation and temperature data from meteorological stations, and the local hydrological bureaus provided precipitation data from rain gauges and runoff data from hydrological stations. The hydrological station closest to the outlet of the Chao River is Xiahui hydrological station, and the Zhangjiafen hydrological station is the closest to

the outlet of the Bai River. Runoff into the MRB is the sum of the runoff amounts measured by both hydrological stations.

The period of study spans 1969 to 2011. This is determined by the availability of data and completeness of records. Precipitation observation starts at 20:00 (Beijing time) the day before and ends at 20:00 [22]. Mean air temperature for a day is the average value of four measured values at 02:00, 08:00, 14:00 and 20:00. The data quality was strictly controlled before their release [23,24]. There are a few missing values in the daily precipitation data. Among the 21 rain gauges, six stations have some missing values (mostly in the non-flood season), but percentage of missing data is less than 4.5%. The missing data were reconstructed by calculating the average value of their neighboring stations [15,25]. Considering relocation and instrument changes of meteorological stations, which may lead to implausible or biased conclusions, the double-mass curve method was adopted to detect the homogeneity of the meteorological data for each station in this study [15,26–28]. After these procedures, 17 rain gauges and nine meteorological stations were retained for the subsequent trend analysis. The spatial distribution of these stations is shown in Figure 1, and their geographical coordinates and elevations are listed in Table 1.

**Table 1.** Hydrological stations, rainfall gauges and meteorological stations used in the study area.

No.	Station Name	Latitude (°N)	Longitude (°E)	Elevation (m)	Category <sup>1</sup>
1	Anchunmengou	40.87	117.20	450	R
2	Baicao	41.12	116.08	990	R
3	Dage	41.18	116.68	620	R
4	Heidaziying	40.92	116.18	740	R
5	Heilongshan	41.25	116.08	1180	R
6	Hushenha	40.88	116.97	350	R
7	Longguan	40.78	115.57	1070	R
8	Maying	41.15	115.65	1130	R
9	Sandaohu	41.13	116.45	730	R
10	Sandaoying	40.78	116.38	540	R
11	Shanghuangqi	41.45	116.67	870	R
12	Shipozi	40.90	116.82	460	R
13	Shirengou	41.07	117.02	480	R
14	Tuchengzi	41.30	116.60	740	R
15	Xiaobazi	41.45	116.37	1045	R
16	Yunzhou Reservoir	41.03	115.77	980	R
17	Zhenanbao	41.12	115.88	1150	R
18	Chicheng	40.88	115.83	867	W <sup>1</sup>
19	Chongli	40.97	115.28	1248	W
20	Fengning	41.22	116.63	661	W
21	Guyuan	41.67	115.67	1412	W
22	Huailai	40.40	115.50	536	W
23	Luanping	40.93	117.33	529	W
24	Miyun	40.38	116.87	71	W
25	Shangdianzi	40.65	117.12	293	W
26	Xinglong	40.40	117.47	633	W
27	Xiahui	40.62	117.17	198	H <sup>1</sup>
28	Zhangjiafen	40.62	116.78	193	H

Note: <sup>1</sup> The letters H, R and W stand for hydrological station, rain gauge and meteorological station, respectively.

Seasonal and annual precipitation amount, mean air temperature and streamflow at the station level and at the basin level were analyzed in this study. Recognizing the annual patterns of these variables in the MRB (Figure 2), in this study we divide the year into flood season and non-flood season. The flood season is from June to September; the non-flood season includes the other months [29]. In addition, three precipitation indices used in this study included precipitation amount, intensity and frequency. Precipitation frequency was calculated by dividing the number of days with precipitation larger than 0.1 mm within a precipitation category by the number of all days with data at annual

and seasonal time scales, and precipitation intensity as the mean precipitation rates averaged over the days with the corresponding precipitation events at the corresponding time scale [30]. Daily precipitation totals  $\geq 0.1$  mm were treated as precipitation event. Observed daily precipitation was classified into four grades of intensity precipitation according to CMA standards in this study: light ( $0.1 \leq p < 10$  mm/day), medium ( $10 \leq p < 25$  mm/day), large ( $25 \leq p < 50$  mm/day) and heavy ( $p > 50$  mm/day) [31]. In order to quantify changes of hydroclimatic variables, several time series of seasonal and annual mean temperature, precipitation amount and streamflow at the station level and at the basin level, seasonal and annual precipitation indices for different precipitation intensities at the basin level were constructed for further analysis. Seasonal and annual observed series for each station, which were calculated from arithmetic average of daily or monthly corresponding measurements, were averaged to derive corresponding seasonal and annual area-average series in the MRB. To explore the spatial distribution of seasonal and annual meteorological variables, inverse distance weighted interpolation based on each individual stations was used due to its good performance in the spatial interpolation of meteorological variables [23].

### 2.3. Methodology

#### 2.3.1. Trend Detection and Slope Estimator

The Mann–Kendall (MK) test, which is a useful nonparametric technique, has been widely used to analyze the significance of monotonic trends in hydrological and meteorological time series [10,32]. This is attributed to the fact that because it does not make any distribution assumption about the test data and has the same power as its parametric competitors [33]. Therefore, the MK test was also employed to investigate the presence of significant trends for hydroclimatic variables of interest in this study. In this study, the statistical significance of the trends was estimated at the significance levels of  $\alpha = 5\%$  and  $1\%$ . When the significance levels are set at 0.01 and 0.05,  $|Z|$  are 2.58 and 1.96, respectively. In addition to trend detection, it is necessary to estimate the trend magnitude. The slope  $\beta$ , developed by Hirsch et al. [34] based on the work of Sen [35], was used in this study as an unbiased estimator of trend magnitude. Detailed introduction to these two methods are available in Xu et al. [10] and Ouarda et al. [4].

#### 2.3.2. Serial Correlation Effect

As the MK test result is sensitive to serial correlation in the time series, especially if there is a positive serial correlation, the time series should be “pre-whitened” to eliminate the effect of serial correlation prior to a trend analysis using the MK test [36–38]. Otherwise, trend might be incorrectly estimated, and the probability of a Type 1 error can increase. The serial correlation analysis method presented by Yue et al. [36] was used to test the presence of serial correlation proposed. Lag-1 serial correlation test was analyzed according to proposal from von Storch [38] and was adopted widely to eliminate the effect of serial correlation [27,28,39,40]. In this study, a trend-free pre-whitening (TFPW) method was used as follows:

1. If the slope is nearly equal to zero, it is not necessary to calculate for trend. Otherwise, the data are detrended by the slope using Sen’s estimator of slope.
2. The lag-1 serial coefficient ( $r_1$ ) of the detrended series is calculated and subtracted from it. After applying this subtraction, the residuals should represent an independent series. A new series was reconstructed based on the linear trend and residuals. This new series can keep the true trend and is no longer affected by the effects of autocorrelation.
3. The MK trend test is applied to the new series to estimate the significance of monotonic trend. The detailed description of serial correlation analysis and the TFPW method can be found in [28,37].

### 3. Results

#### 3.1. Serial Correlation of the Hydroclimatic Data

Autocorrelation test results for mean temperature and precipitation during the annual, in flood season and in non-flood season at all stations and at the basin scale are shown in Figure 3. Regarding time series of mean temperature, positive serial correlations were obtained, except stations 20, 21, and 22, and basin mean temperature. Annual mean temperature series at stations 1, 3, 5, and 9, and non-flood temperature series at stations 19, 20 and 21 had a significant correlation, respectively. For precipitation, a mix of positive and negative serial correlations was obtained. The positive serial correlation was significant only for flood season precipitation at station 26. In addition, non-flood streamflow also has significant positive correlation. Accordingly, these time series with significant positive serial correlation should be removed before trend test.

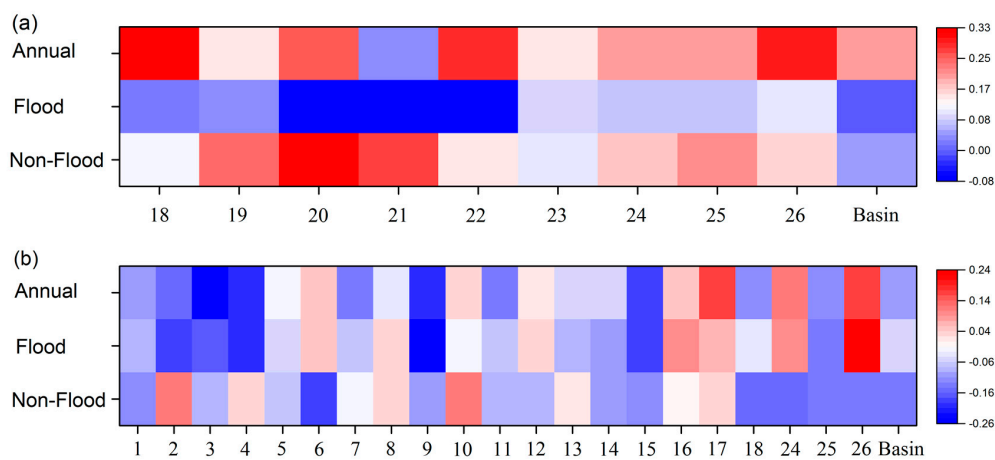


**Figure 3.** Lag-1 serial correlation coefficients for the: (a) mean temperature; and (b) precipitation at the station level and at the basin level.

#### 3.2. Temperature

The variation in observed mean temperature during the year, in the flood season, and in the non-flood season from 1969 to 2011 is presented in Figure 4. The mean temperatures in the MRB were 7.45 °C, 19.98 °C and 1.20 °C, respectively, during the year, in flood season and in non-flood season.

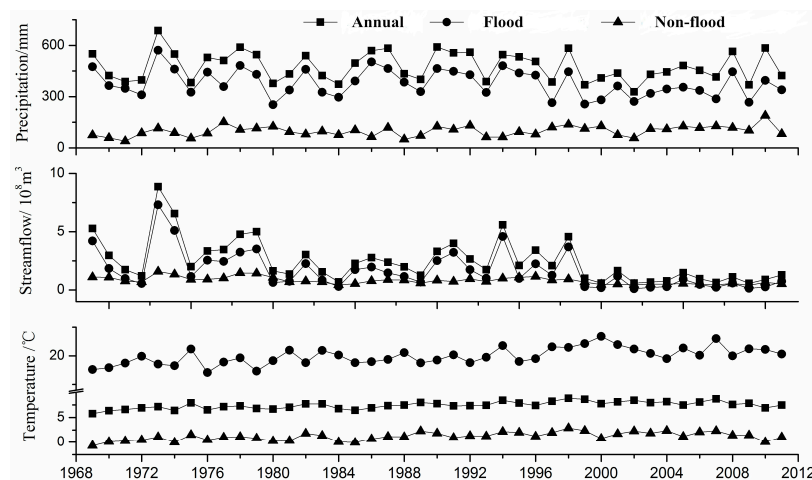


**Figure 4.** Time series of annual, flood and non-flood precipitation, streamflow and temperature from 1969 to 2011.

As indicated by Table 2, overall the average annual temperature exhibited a significantly increasing trend at the  $\alpha = 0.01$  level with a magnitude of  $0.36\text{ }^{\circ}\text{C}/10$  years for the past 43 years. The mean temperatures during the flood and non-flood seasons also followed this increasing trend at rates of  $0.32\text{ }^{\circ}\text{C}/10$  years and  $0.38\text{ }^{\circ}\text{C}/10$  years at the same significance level, respectively. The magnitude of the increase in mean temperature in the non-flood season was slightly greater than that in the flood season, leading to a decrease in intra-annual temperature range. This showed that the climate of the MRB is warming over the past 43 years. Figure 5a shows that the average annual temperature gradually decreased from southeast to northwest, which was related to the basin topography that increases in elevation from southeast to northwest (Figure 1). The spatial distributions of mean temperature in flood and non-flood seasons were omitted because they were similar to that of mean annual temperature.

**Table 2.** Trend magnitudes for annual, flood and non-flood precipitation, temperature and total runoff from 1969 to 2011 in the MRB.

Variables	Trend Magnitude <sup>1</sup>		
	Annual	Flood	Non-Flood
Precipitation	−11.00	−18.50 *	6.91 *
Temperature	0.36 **	0.32 **	0.38 **
Total runoff	−1.60 **	−1.12 **	−0.42 **

Notes: <sup>1</sup> The units for precipitation, temperature and runoff are mm/10 years,  $^{\circ}\text{C}/10$  years and  $10^8\text{ m}^3/10$  years, respectively; \* indicates statistically significant at  $\alpha = 0.05$  level; \*\* indicates statistically significant at  $\alpha = 0.01$  level.

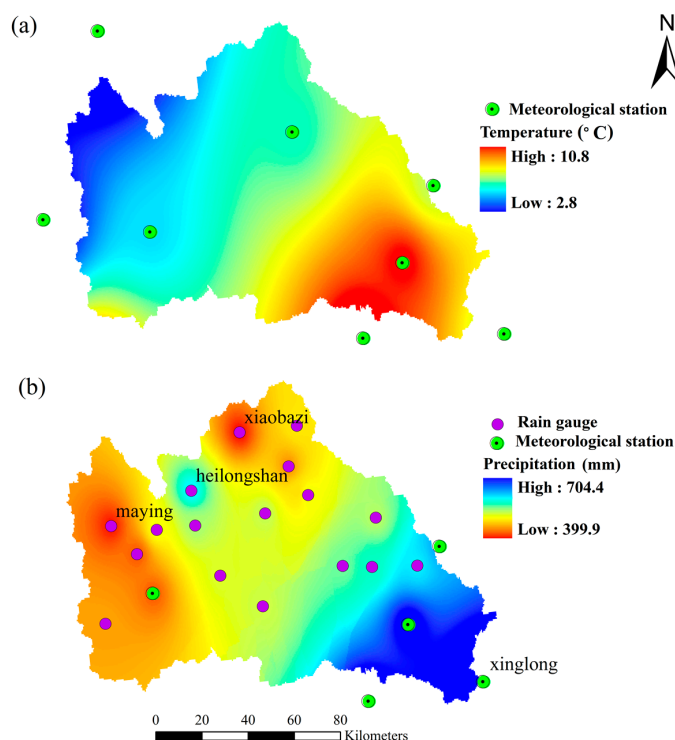


**Figure 5.** Spatial distributions of: (a) annual mean temperature; and (b) precipitation in the MRB.

Figure 6 shows the results of spatial distributions of Mann–Kendall’s test and trend magnitudes of annual, flood and non-flood mean temperature for nine meteorological stations in and around the MRB. All stations exhibited statistically significant increasing trends for annual, flood and non-flood mean temperature: the increasing trends for eight stations were significant at the level of  $\alpha = 0.01$  and an increasing trend for the remaining station (Luanping station) at the  $\alpha = 0.05$  significance level.

The trend magnitude of mean temperature during the year, in the flood season and in the non-flood season varied slightly among different stations. The majority of the basin has a trend magnitude of annual mean temperature at 0.25–0.40 °C/10 years. Figure 6 also indicates that the trend magnitude of mean temperature generally decreased from southeast to northwest. Mean temperature experienced the largest increasing trend in the west mountainous region. In other words, the region with lower mean temperature had higher warming rate in the MRB. The flood and non-flood seasons had almost similar spatial distribution of trend magnitude of mean temperature to that during the year (Figure 6).

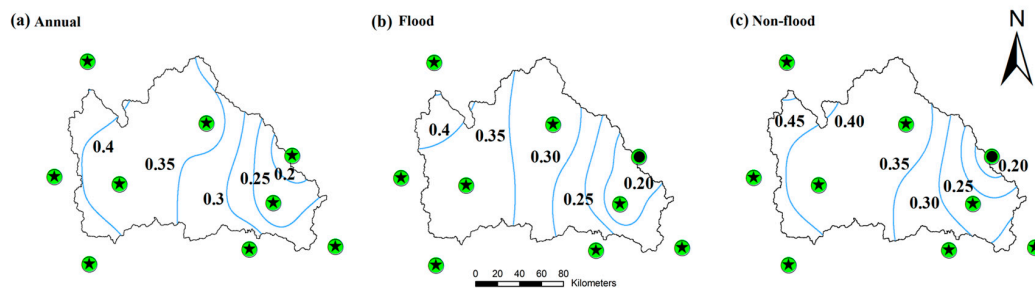


**Figure 6.** Spatial distributions of trend magnitudes for: (a) annual; (b) flood; and (c) non-flood mean temperature in the MRB. Green solid circles denote upward trend. Circles with a black dot and five-pointed star stand for significant trends at  $\alpha = 0.05$  and  $0.01$  significance levels, respectively.

### 3.3. Precipitation

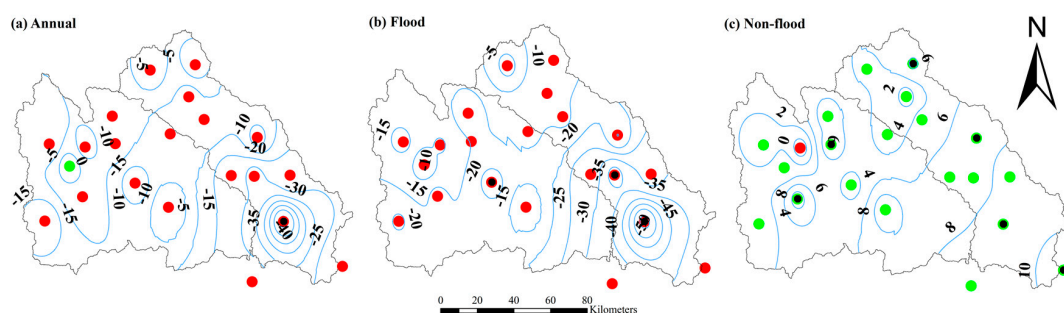
#### 3.3.1. Spatial and Temporal Precipitation Changes

Figure 4 shows that the annual, flood and non-flood average precipitation in the MRB were 477 mm, 378 mm, and 98 mm from 1969 to 2011, respectively. With regard to precipitation, Table 2 shows that the precipitation trends in the flood and non-flood seasons were opposite: the former featured a significant decreasing trend at a magnitude of 18.50 mm/10 years at the level of  $\alpha = 0.05$ , whereas the latter exhibited a significant increasing trend at an average rate of 6.91 mm/10 years. Annual precipitation showed a decreasing trend without statistical significance at the level of  $\alpha = 0.05$ , probably due to the opposing nature of the trends in the flood and non-flood seasons. The difference in precipitation amount between flood and non-flood seasons has decreased over the past 43 years.

The spatial distribution of average precipitation (1969–2011) during the year, in flood season, and in non-flood season is shown in Figure 5b. The overall spatial distribution of annual precipitation shows that precipitation decreased from southeast to northwest, ranging from 400 mm to 704 mm, which was related to the orographic factor (Figure 1). Xinglong station were located in the rain-rich regions (approximately 660 mm) downstream of the watershed, but the areas, where the Xiaobazi and Maying rain gauges are located, received the lowest precipitation (approximately 390 mm). In addition, another high precipitation zone (approximately 520 mm) is located near the Heilongshan rain gauge in the upstream part of the basin. The flood season and non-flood season precipitation exhibited similar spatial distribution to annual precipitation and varied from 255 mm to 576 mm and from 50 mm to 185 mm, respectively.

The spatial distribution of trend magnitudes of annual, flood season and non-flood season precipitation for all stations in Table 1 was visually presented by plotting the results on maps of the study area (Figure 7). As for annual precipitation (Figure 7a), 20 out of 21 stations in the basin exhibited decreasing trends, but only shangdianzi station showed a significant decreasing trend at the level of  $\alpha = 0.05$ . Only one station in the upstream part of the basin exhibited non-significant precipitation increases. As for flood season precipitation (Figure 7b), decreasing trends prevailed in the entire basin. Among all stations, three stations (14.3%) showed significant downward trends at the  $\alpha = 0.05$  level. With respect to non-flood season precipitation (Figure 7c), increasing trends dominated in the entire basin. Six stations were characterized by significant upward trends at

the  $\alpha = 0.05$  level. In addition, only one stations showed a non-significant decreasing trend. It is apparent that stations characterized by higher values of precipitation trend magnitude were located mainly in the lower reaches of the basin. For example, the stations with trend magnitudes of annual, flood season and non-flood season precipitation greater than 20 mm/10 years, 25 mm/10 years and 8 mm/10 years, respectively, were located mainly in the downstream part of the basin. Moreover, the number of stations showing significant precipitation trends at the 0.05 level over the Chao River sub-basin was greater than in the Bai River sub-basin, indicating that precipitation change in the Chao River sub-basin was slightly greater than in the Bai River sub-basin. In addition, the spatial distributions of precipitation trend magnitude for all stations at different time-scales exhibited the same patterns of the decrease from southeast to northwest.



**Figure 7.** Spatial distributions of trend magnitudes for: (a) annual; (b) flood; and (c) non-flood precipitation in the MRB. Red and green solid circles denote downward and upward trends, respectively. Circles with a black dot stand for significant trends at  $\alpha = 0.05$  significance level.

### 3.3.2. Changes in Precipitation Indices

The results shown in Table 3 indicated that precipitation frequency featured a significant decreasing trend in the flood season at the level of  $\alpha = 0.05$  with a magnitude of 1.5 days/10 years and was not-significant decreasing during the year. The rising trend of precipitation frequency in the non-flood season was also non-significant. However, precipitation amount was influenced not only by precipitation frequency, but also by average daily precipitation intensity. The precipitation intensities during the year and in the flood season followed non-significant downward trends, whereas the precipitation intensity in the non-flood season featured an upward trend without statistical significance.

**Table 3.** Trend magnitudes for annual, flood and non-flood precipitation intensity and precipitation frequency from 1969 to 2011 in the MRB.

Variables	Trend Magnitude <sup>1</sup>		
	Annual	Flood	Non-Flood
Precipitation intensity	−0.12	−0.23	0.14
Precipitation frequency	−0.88	−1.50 *	0.43

Notes: <sup>1</sup> The units of trend magnitudes for precipitation frequency and precipitation intensity are day/10 years and mm/day/10 years, respectively; \* indicates statistically significant at  $\alpha = 0.05$  level.

For different precipitation grades, precipitation amount ranking in the descending order during the year matches that in the flood season, and the ranking is medium, light, large and heavy rain. The first three categories of precipitation accounted for more than 90% of precipitation. Precipitation during non-flood season was composed of light, medium, large and heavy rain in descending order. Similarly, the ranking for precipitation frequency during the year, in flood season and in non-flood season was the same; the first two categories were light and medium rain, which accounted for more than 85% of precipitation frequency (Supplementary Materials Figure S1).

The Mann–Kendall trend test results of three precipitation indices for the different precipitation grades in the basin during the year, in the flood season and non-flood season are shown in Table 4. Because heavy rain was rare, not all the magnitudes of change in precipitation intensity and frequency for heavy rain were analyzed. Flood precipitation intensity for large rain and non-flood precipitation amount for medium rain showed significant increasing trends at the level of  $\alpha = 0.05$ , their magnitude were 0.40 mm/day/10 years and 3.37 mm/10 years, respectively.

**Table 4.** Trend magnitudes for precipitation amount, precipitation frequency and precipitation intensity for different precipitation grades in the MRB.

Variables	Trend Magnitude <sup>1</sup>								
	Annual			Flood			Non-Flood		
	PA	PF	PI	PA	PF	PI	PA	PF	PI
Light	−0.20	−0.19	0.02	−2.80	−0.70	0.00	1.59	0.15	0.06
Medium	−3.67	−0.18	0.00	−6.70	−0.40	0.00	3.37 *	0.21	0.10
Large	−4.11	−0.13	0.15	−6.50	−0.20	0.40 *	0.70	0.00	0.60
Heavy	−4.28	−0.06	−0.97	−3.80	0.00	−1.00			

Notes: <sup>1</sup> The units of trend magnitudes for precipitation amount, precipitation frequency and precipitation intensity are mm/day/10 years, days/10 years, and mm/day/10 years, respectively; \* indicates statistically significant at  $\alpha = 0.05$  level.

### 3.4. Streamflow

Figure 8 shows the variation in observed mean streamflow during the year, in flood season and in non-flood season from 1969 to 2011. Annual, flood and non-flood mean streamflow in the MRB were  $2.46 \times 10^8 \text{ m}^3$ ,  $1.66 \times 10^8 \text{ m}^3$ , and  $0.80 \times 10^8 \text{ m}^3$ , respectively. The runoff amount during the flood season accounted for almost 70% of the annual total in the basin (Figure 2). As shown in Table 2 and Figure 8, the annual streamflow for the entire basin exhibited a continuous and statistically significant decreasing trend with a rate of  $1.6 \times 10^8 \text{ m}^3/10 \text{ years}$  at the  $\alpha = 0.01$  significance level. Meanwhile, the flood season and non-flood season streamflow also showed declining trends with magnitudes of approximately  $1.1 \times 10^8 \text{ m}^3/10 \text{ years}$  and  $0.40 \times 10^8 \text{ m}^3/10 \text{ years}$ , respectively. The trend magnitude of flood season precipitation was higher than that of non-flood season precipitation, indicating that change in the runoff amount during the flood season dominated the change in the annual runoff amount. The runoff coefficient, which is defined as the ratio of annual streamflow to precipitation, showed a significant decreasing trend with a Z value of  $-4.87$  from 1969 to 2011 (Figure 7). The decreased streamflow was more obvious after 2000 than before.

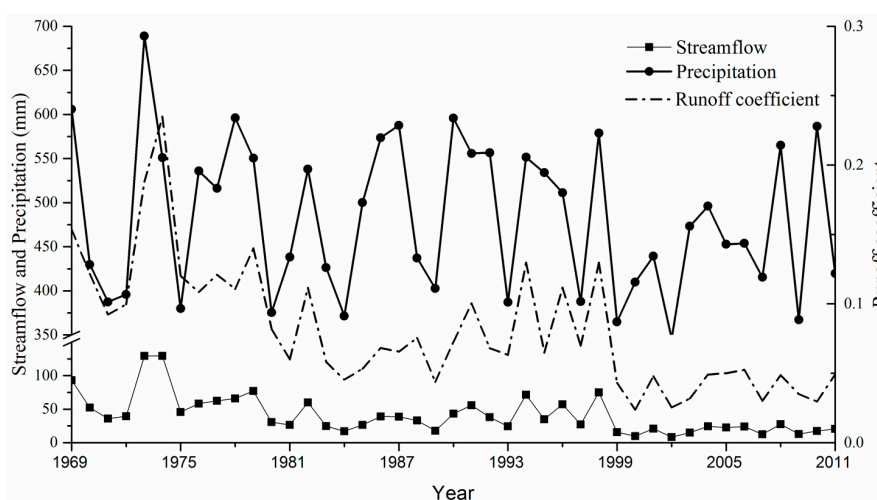


**Figure 8.** Time series of annual precipitation, streamflow and runoff coefficient in the MRB.

## 4. Discussion

### 4.1. Attribution Analysis

The trend test in this study revealed that climate has become warmer and tended to be drier in the MRB during the past 43 years. The trend magnitude of mean annual temperature in the MRB was 0.36 °C/10 years during 1969–2011, which was close to the values of 0.34 °C/10 years over the Haihe River Basin during 1960–2010 [41] and 0.38 °C/10 years in China during 1979–2007 [42]. The analysis presented here demonstrated that the mean annual temperature in the MRB has increased by 1.55 °C over the past 43 years, and this increase was greater than in the Haihe River Basin and at the global level (0.72 °C during 1951–2012) [43]. The trends of air temperature may result from global warming due to the greenhouse effect, urban heat island effect and long-term climate variability [44]. Due to the presence of the urban heat island caused by urban expansion, the warming trend can be overestimated. Shao et al. [42] concluded that, from 1970 to 2007, warming rate of mean temperature in China was about 1.58 °C, of which about 0.01 °C was attributed to urban heat island effect, with a peak of 0.09 °C in several regions. Compared to the increase in mean temperature, the overestimation caused by urban heat island effect is small. Therefore, it can be inferred that some of the warming trend in the MRB is a result of global warming. There is also seasonal difference in trend magnitude for mean temperature. Specifically, the trend magnitude in non-flood season is higher than in flood season. This may be attributed to the higher warming rate in winter (from December to January) compared to spring, summer and autumn. GuoLi and GuoYu [45] indicated that, in China, warming rate in winter was the highest over the past 50 years (1951–2001). Xu et al. [10] also found that the strongest increase in winter temperature occurred in the Tarim River basin from 1960 to 2007. The strongest increase of mean temperature in winter might have something to do with the large quantity of CO<sub>2</sub> and N<sub>2</sub>O emissions during the heating period (from November to March) [46].

The area-averaged annual precipitation has shown a non-significant decreasing trend ( $\alpha > 0.1$ ) in the last 43 years. This result was different from that reported by Ma et al. [16]. They found that annual precipitation had a significant decreasing trend ( $\alpha = 0.1$ ) from 1956 to 2005 in the MRB. This difference can be attributed to the following factors: (1) time span of data; (2) the number of stations used; and (3) data processing method [28]. For the intra-annual distribution of precipitation, the significantly decreased flood season precipitation, accounting for more than 70% of annual precipitation, resulted in a decrease in annual precipitation. Decreased precipitation frequency might be the major cause of the decrease in flood precipitation. The dynamic mechanism of changes in regional precipitation is complicated. The main factors include warming of the surface and lower troposphere, changes in the atmospheric circulation, changes in soil moisture, changes in the concentration of anthropogenic aerosols and land use and land cover change [47–50]. In the Haihe River Basin, the summer precipitation is mainly controlled by the East Asian monsoon. Thus, the decrease in flood precipitation may be related to the weaker summer monsoon in the East Asia region since the 1970s [51,52]. In addition, anthropogenic aerosols have been an important factor. Specifically, the impact of anthropogenic aerosols on the decrease in precipitation was remarkable in summer and was possibly caused by the influence of aerosols on convective precipitation in North China [50]. Daniels et al. [49] used a regional climate model to simulate the effect of land use changes on precipitation in the Netherlands, and found that the simulated effects of land use changes on precipitation in summer are smaller than the effects of climate change, but are not negligible. Thus, it is difficult to directly compare the variations in precipitation indices in the MRB to other studies. In our study, only flood precipitation intensity for large rain and non-flood precipitation amount for medium rain showed statistically significantly increasing trends which might be partly attributed to the thermodynamic effect of a warmer atmosphere being able to carry more water vapour [48]. The annual, flood season and non-flood season streamflow showed significant decreasing trends in the watershed, which was consistent with the results from Bao et al. [18], Ma et al. [16], and Wang et al. [21]. Within the watershed, the intra-annual distribution of streamflow was in agreement with that of precipitation and the change

tendency of annual streamflow was in line with that of annual precipitation in the basin because of precipitation-driven hydrologic processes (Figure 8). However, the decline in streamflow was greater than that of precipitation. In other words, the straight-line slope of annual streamflow was  $-1.36$  mm/year, which is greater than  $-1.25$  mm/year for precipitation. Meanwhile, the trend in the runoff coefficient also decreased significantly. Hence, the relationship between annual precipitation and streamflow showed a non-stationary state in the basin. A faster decrease in runoff than precipitation in the watershed indicated that, in addition to precipitation factor, increased temperature and intensive human activities were also important factors [53,54]. Ma et al. [16] pointed out that the contribution of climate change (precipitation and temperature and human activity to the decreased streamflow was about 55% and 51%, respectively. The human activities include direct withdrawal of water, land use and land cover changes, and construction of hydraulic engineering. Since 1978, China's land reform has motivated farmers to increase farm area to raise their production, causing an increase in agricultural water use from rivers and reservoirs (Yunzhou and Baihepu Reservoirs). In the early 1980s, a soil-water conservation program, including reforestation and other soil-water conservation measures, was implemented in the basin. The average annual reservoir extractions increased from 2.2 mm (runoff depth) from 1956 to 1983 to 13.4 mm from 1984 to 2005. The latter accounted for 23% of the decrease in inflow into the reservoir.

Despite a significant increase in non-flood precipitation characterized by increase in medium rain, the runoff showed a significantly decreasing trend in the non-flood season. This phenomenon might indicate that the increase in medium rain has not increased enough to generate runoff in semi-arid areas, such as the MRB [55].

#### 4.2. Implications for Watershed Management

Historical hydroclimatic observed data are always useful for planning and designing water resource projects [56]. The non-stationary relationship between annual precipitation and streamflow should receive more attention from water resources engineers in the context of global warming. Non-point pollution is one of the main causes of eutrophication in the Miyun Reservoir. Hence, reducing non-point pollutants is essential to ensure drinking-water safety for Beijing City [57,58]. Based on the spatial distribution of mean annual precipitation coupled with regional land use and agricultural management practices, potential areas for nutrient loss could be identified, providing guidelines for control measures to minimize nutrient loss. The climate changes in the watershed identified in this study, such as changes in the trend and magnitude of precipitation and temperature could be used as a reference for studies related to climate change impact in the watershed [59]. In flood season, increased precipitation intensity for large rain might mean an increasing probability of flood occurrence and may provide information for water resource management in the watershed.

### 5. Conclusions

The spatial and temporal changes of precipitation, mean temperature, and runoff during 1969–2011 were identified in the MRB in the context of global climate change.

The results in this study revealed that climate has become warmer and tended to be drier in the MRB during the past 43 years. Warming rate in the MRB was in line with the warming trend over the Haihe River Basin during 1960–2010. Although annual precipitation had a non-significant decreasing trend, flood precipitation trend was significant decreasing, and non-flood precipitation trend was significant increasing. Spatial variation in trend magnitude of mean temperature and precipitation were different. For temperature, trend magnitude decreased from southeast to northwest; trend magnitude of precipitation was opposite. The streamflow showed significant decreasing trends at all three time-scales. A non-stationary relationship existed between annual precipitation and streamflow. It is important to not only regard mean precipitation changes but also different precipitation indices for different precipitation intensities to get further insight into the mechanisms behind observed precipitation changes.

The results from this study could be used as a reference for water resource planning and management to maintain the health of the river system and to protect the regional eco-environmental system, especially under future global warming scenarios. In particular, these findings could provide supportive information for: (1) research into the effect of historical climate changes on runoff in the MRB; (2) soil erosion control; and (3) non-point pollution control.

**Supplementary Materials:** The following are available online at [www.mdpi.com/2073-4441/9/2/78/s1](http://www.mdpi.com/2073-4441/9/2/78/s1), Figure S1: Distribution of precipitation (left) and rainy day (right) for different precipitation grades.

**Acknowledgments:** This study was supported by the National Science Foundation for Innovative Research Group (No. 51421065) and the National Science Foundation for Distinguished Young Scholars (No. 51579011).

**Author Contributions:** All authors contributed to the design and development of this manuscript. Tiezhu Yan gathered the data information, performed the data analysis and prepared the first draft of the manuscript. Zhenyao Shen provided the original ideas and improved the discussion. Jian Wen Bai edited the manuscript prior to submission.

**Conflicts of Interest:** The authors declare no conflict of interest.

## References

1. Meinshausen, M.; Meinshausen, N.; Hare, W.; Raper, S.C.B.; Frieler, K.; Knutti, R.; Frame, D.J.; Allen, M.R. Greenhouse-gas emission targets for limiting global warming to 2 °C. *Nature* **2009**, *458*, 1158–1163. [[CrossRef](#)] [[PubMed](#)]
2. Ye, L.; Grimm, N.B. Modelling potential impacts of climate change on water and nitrate export from a mid-sized, semiarid watershed in the US Southwest. *Clim. Chang.* **2013**, *120*, 419–431. [[CrossRef](#)]
3. Jha, M.K.; Gassman, P.W.; Panagopoulos, Y. Regional changes in nitrate loadings in the Upper Mississippi River Basin under predicted mid-century climate. *Reg. Environ. Chang.* **2015**, *15*, 449–460. [[CrossRef](#)]
4. Ouarda, T.B.M.J.; Charron, C.; Kumar, K.N.; Marpu, P.R.; Ghedira, H.; Molini, A.; Kayal, I. Evolution of the rainfall regime in the United Arab Emirates. *J. Hydrol.* **2014**, *514*, 258–270. [[CrossRef](#)]
5. Mbungu, W.; Ntegeka, V.; Kahimba, F.C.; Taye, M.; Willems, P. Temporal and spatial variations in hydro-climatic extremes in the Lake Victoria basin. *Phys. Chem. Earth* **2012**, *50–52*, 24–33. [[CrossRef](#)]
6. Fu, G.B.; Chen, S.L.; Liu, C.M.; Shepard, D. Hydro-climatic trends of the Yellow River Basin for the last 50 years. *Clim. Chang.* **2004**, *65*, 149–178. [[CrossRef](#)]
7. Chen, J.; Wu, X.; Finlayson, B.L.; Webber, M.; Wei, T.; Li, M.; Chen, Z. Variability and trend in the hydrology of the Yangtze River, China: Annual precipitation and runoff. *J. Hydrol.* **2014**, *513*, 403–412. [[CrossRef](#)]
8. Huntington, T.G.; Billmire, M. Trends in precipitation, runoff, and evapotranspiration for rivers draining to the gulf of maine in the United States. *J. Hydrometeorol.* **2014**, *15*, 726–743. [[CrossRef](#)]
9. Bao, Z.; Zhang, J.; Liu, J.; Wang, G.; Yan, X.; Wang, X.; Zhang, L. Sensitivity of hydrological variables to climate change in the Haihe River Basin, China. *Hydrol. Process.* **2012**, *26*, 2294–2306. [[CrossRef](#)]
10. Xu, Z.X.; Liu, Z.F.; Fu, G.B.; Chen, Y.N. Trends of major hydroclimatic variables in the Tarim River Basin during the past 50 years. *J. Arid Environ.* **2010**, *74*, 256–267. [[CrossRef](#)]
11. Chen, Y.; Guan, Y.; Shao, G.; Zhang, D. Investigating trends in streamflow and precipitation in Huangfuchuan Basin with wavelet analysis and the Mann-Kendall test. *Water* **2016**, *8*, 77. [[CrossRef](#)]
12. Yeh, C.-F.; Wang, J.; Yeh, H.-F.; Lee, C.-H. Spatial and temporal streamflow trends in Northern Taiwan. *Water* **2015**, *7*, 634–651. [[CrossRef](#)]
13. Brunetti, M.; Maugeri, M.; Nanni, T. Changes in total precipitation, rainy days and extreme events in Northeastern Italy. *Int. J. Climatol.* **2001**, *21*, 861–871. [[CrossRef](#)]
14. Chou, C.; Chen, C.-A.; Tan, P.-H.; Chen, K.T. Mechanisms for global warming impacts on precipitation frequency and intensity. *J. Clim.* **2012**, *25*, 3291–3306. [[CrossRef](#)]
15. Zhang, Q.; Singh, V.P.; Peng, J.; Chen, Y.D.; Li, J. Spatial-temporal changes of precipitation structure across the Pearl River Basin, China. *J. Hydrol.* **2012**, *440–441*, 113–122. [[CrossRef](#)]
16. Ma, H.A.; Yang, D.W.; Tan, S.K.; Gao, B.; Hu, Q.F. Impact of climate variability and human activity on streamflow decrease in the Miyun Reservoir Catchment. *J. Hydrol.* **2010**, *389*, 317–324. [[CrossRef](#)]
17. Yang, Y.; Tian, F. Abrupt change of runoff and its major driving factors in Haihe River Catchment, China. *J. Hydrol.* **2009**, *374*, 373–383. [[CrossRef](#)]

18. Bao, Z.X.; Fu, G.B.; Wang, G.Q.; Jin, J.L.; He, R.M.; Yan, X.L.; Liu, C.S. Hydrological projection for the Miyun Reservoir Basin with the impact of climate change and human activity. *Quat. Int.* **2012**, *282*, 96–103. [[CrossRef](#)]
19. Zheng, J.K.; Sun, G.; Li, W.H.; Yu, X.X.; Zhang, C.; Gong, Y.B.; Tu, L.H. Impacts of land use change and climate variations on annual inflow into the Miyun Reservoir, Beijing, China. *Hydrol. Earth Syst. Sci.* **2016**, *20*, 1561–1572. [[CrossRef](#)]
20. Tang, L.; Yang, D.; Hu, H.; Gao, B. Detecting the effect of land-use change on streamflow, sediment and nutrient losses by distributed hydrological simulation. *J. Hydrol.* **2011**, *409*, 172–182. [[CrossRef](#)]
21. Wang, X.; Hao, G.; Yang, Z.; Liang, P.; Cai, Y.; Li, C.; Sun, L.; Zhu, J. Variation analysis of streamflow and ecological flow for the twin rivers of the Miyun Reservoir Basin in Northern China from 1963 to 2011. *Sci. Total Environ.* **2015**, *536*, 739–749. [[CrossRef](#)] [[PubMed](#)]
22. Zhang, X.; Cong, Z. Trends of precipitation intensity and frequency in hydrological regions of China from 1956 to 2005. *Glob. Planet. Chang.* **2014**, *117*, 40–51. [[CrossRef](#)]
23. Huang, S.; Huang, Q.; Zhang, H.; Chen, Y.; Leng, G. Spatio-temporal changes in precipitation, temperature and their possibly changing relationship: A case study in the Wei River Basin, China. *Int. J. Climatol.* **2016**, *36*, 1160–1169. [[CrossRef](#)]
24. Liu, B.H.; Xu, M.; Henderson, M.; Qi, Y. Observed trends of precipitation amount, frequency, and intensity in China, 1960–2000. *J. Geophys. Res.* **2005**, *110*. [[CrossRef](#)]
25. Wang, W.; Xing, W.; Yang, T.; Shao, Q.; Peng, S.; Yu, Z.; Yong, B. Characterizing the changing behaviours of precipitation concentration in the Yangtze River Basin, China. *Hydrol. Process.* **2013**, *27*, 3375–3393. [[CrossRef](#)]
26. Tabari, H.; Somee, B.S.; Zadeh, M.R. Testing for long-term trends in climatic variables in Iran. *Atmos. Res.* **2011**, *100*, 132–140. [[CrossRef](#)]
27. Gocic, M.; Trajkovic, S. Analysis of changes in meteorological variables using Mann-Kendall and Sen's slope estimator statistical tests in Serbia. *Glob. Planet. Chang.* **2013**, *100*, 172–182. [[CrossRef](#)]
28. Chattopadhyay, S.; Edwards, D.R. Long-term trend analysis of precipitation and air temperature for Kentucky, United States. *Climate* **2016**, *4*, 1–10. [[CrossRef](#)]
29. Wang, H.Q.; Zhang, M.S.; Zhu, H.; Dang, X.Y.; Yang, Z.; Yin, L.H. Hydro-climatic trends in the last 50 years in the lower reach of the Shiyang River Basin, NW China. *Catena* **2012**, *95*, 33–41. [[CrossRef](#)]
30. Sun, Y.; Solomon, S.; Dai, A.; Portmann, R.W. How often will it rain? *J. Clim.* **2007**, *20*, 4801–4818. [[CrossRef](#)]
31. Fu, C.; Dan, L. Trends in the different grades of precipitation over South China during 1960–2010 and the possible link with anthropogenic aerosols. *Adv. Atmos. Sci.* **2014**, *31*, 480–491. [[CrossRef](#)]
32. Feng, X.; Zhang, G.; Yin, X. Hydrological responses to climate change in Nenjiang River Basin, Northeastern China. *Water Resour. Manag.* **2011**, *25*, 677–689. [[CrossRef](#)]
33. Yue, S.; Pilon, P. A comparison of the power of the t test, Mann-Kendall and bootstrap tests for trend detection. *Hydrol. Sci. J.* **2004**, *49*, 21–37. [[CrossRef](#)]
34. Hirsch, R.M.; Slack, J.R.; Smith, R.A. Techniques of trend analysis for monthly water-quality data. *Water Resour. Res.* **1982**, *18*, 107–121. [[CrossRef](#)]
35. Sen, P.K. Estimates of the regression coefficient based on Kendall's tau. *J. Am. Stat. Assoc.* **1968**, *63*, 1379–1389. [[CrossRef](#)]
36. Yue, S.; Pilon, P.; Phinney, B.; Cavadias, G. The influence of autocorrelation on the ability to detect trend in hydrological series. *Hydrol. Process.* **2002**, *16*, 1807–1829. [[CrossRef](#)]
37. Yue, S.; Wang, C.Y. Applicability of prewhitening to eliminate the influence of serial correlation on the Mann-Kendall test. *Water Resour. Res.* **2002**, *38*, 1–7. [[CrossRef](#)]
38. Von Storch, H. Misuses of statistical analysis in climate research. In *Analysis of Climate Variability: Applications of Statistical Techniques*; von Storch, H., Navarra, A., Eds.; Springer: Berlin/Heidelberg, Germany, 1995; pp. 11–26.
39. Sayemuzzaman, M.; Jha, M.K. Seasonal and annual precipitation time series trend analysis in North Carolina, United States. *Atmos. Res.* **2014**, *137*, 183–194. [[CrossRef](#)]
40. Partal, T.; Kahya, E. Trend analysis in Turkish precipitation data. *Hydrol. Process.* **2006**, *20*, 2011–2026. [[CrossRef](#)]
41. Wang, Y.C.; Sun, Y.L.; Zhang, J.; Wang, Z.L. Climate change characteristics of Haihe River Basin in recent 51 years. *J. Tianjin Norm. Univ.* **2014**, *34*, 58–63. (In Chinese)

42. Shao, Q.; Sun, C.; Liu, J.; He, J.; Kuang, W.; Tao, F. Impact of urban expansion on meteorological observation data and overestimation to regional air temperature in China. *J. Geogr. Sci.* **2011**, *21*, 994. [[CrossRef](#)]
43. Intergovernmental Panel on Climate Change. *Climate Change 2013: The Physical Science Basis, In the Fifth Assessment Report of the Intergovernmental Panel on Climate Change*; Cambridge University Press: Cambridge, UK; New York, NY, USA, 2013.
44. Qin, N.X.; Chen, X.; Fu, G.B.; Zhai, J.Q.; Xue, X.W. Precipitation and temperature trends for the Southwest China: 1960–2007. *Hydrol. Process.* **2010**, *24*, 3733–3744. [[CrossRef](#)]
45. Tang, G.L.; Ren, G.Y. Reanalysis of surface air temperature change of the last 100 years over China. *Clim. Environ. Res.* **2005**, *10*, 791–798. (In Chinese)
46. Yin, Y.Y.; Liu, H.; Yi, X.S.; Liu, W.D. Spatiotemporal variation and abrupt change analysis of temperature from 1960 to 2012 in the Huang-Huai-Hai Plain, China. *Adv. Meteorol.* **2015**, *2015*, 1–11. [[CrossRef](#)]
47. Schneider, T.; O’Gorman, P.A.; Levine, X.J. Water vapor and the dynamics of climate changes. *Rev. Geophys.* **2010**, *48*. [[CrossRef](#)]
48. Kendon, E.J.; Rowell, D.P.; Jones, R.G. Mechanisms and reliability of future projected changes in daily precipitation. *Clim. Dyn.* **2010**, *35*, 489–509. [[CrossRef](#)]
49. Daniels, E.; Lenderink, G.; Hutjes, R.; Holtslag, A. Relative impacts of land use and climate change on summer precipitation in the Netherlands. *Hydrol. Earth Syst. Sci.* **2016**, *20*, 4129–4142. [[CrossRef](#)]
50. Duan, J.; Mao, J. Influence of aerosol on regional precipitation in North China. *Chin. Sci. Bull.* **2009**, *54*, 474–483. [[CrossRef](#)]
51. Ding, Y.; Ren, G.; Zhao, Z.; Xu, Y.; Luo, Y.; Li, Q.; Zhang, J. Detection, causes and projection of climate change over China: An overview of recent progress. *Adv. Atmos. Sci.* **2007**, *24*, 954–971. [[CrossRef](#)]
52. Zhou, T.; Gong, D.; Li, J.; Li, B. Detecting and understanding the multi-decadal variability of the east Asian summer monsoon—Recent progress and state of affairs. *Meteorol. Z.* **2009**, *18*, 455–467.
53. Ren, L.L.; Wang, M.R.; Li, C.H.; Zhang, W. Impacts of human activity on river runoff in the northern area of China. *J. Hydrol.* **2002**, *261*, 204–217. [[CrossRef](#)]
54. Lu, S.L.; Wu, B.F.; Wei, Y.P.; Yan, N.N.; Wang, H.; Guo, S.Y. Quantifying impacts of climate variability and human activities on the hydrological system of the Haihe River Basin, China. *Environ. Earth Sci.* **2015**, *73*, 1491–1503. [[CrossRef](#)]
55. Wang, X.; Wang, J.; Ou, Y.; Yu, Y. Phosphorus loss from soil-runoff-sediment at slope plots. *J. Soil Water Conserv.* **2008**, *22*, 1–5.
56. Chen, H.; Guo, S.; Xu, C.-Y.; Singh, V.P. Historical temporal trends of hydro-climatic variables and runoff response to climate variability and their relevance in water resource management in the Hanjiang Basin. *J. Hydrol.* **2007**, *344*, 171–184. [[CrossRef](#)]
57. Jiao, J.; Du, P.F.; Lang, C. Nutrient concentrations and fluxes in the upper catchment of the Miyun Reservoir, China, and potential nutrient reduction strategies. *Environ. Monit. Assess.* **2015**, *2015*, 110–125. [[CrossRef](#)] [[PubMed](#)]
58. Wang, X.; Li, T.; Xu, Q.; He, W. Study of the distribution of non-point source pollution in the watershed of the Miyun Reservoir, Beijing, China. *Water Sci. Technol.* **2001**, *44*, 35–40. [[PubMed](#)]
59. Bouraoui, F.; Grizzetti, B.; Granlund, K.; Rekolainen, S.; Bidoglio, G. Impact of climate change on the water cycle and nutrient losses in a Finnish catchment. *Clim. Chang.* **2004**, *66*, 109–126. [[CrossRef](#)]

